Integrated Photonic Devices and Materials

Academic and Research Staff
Professor Leslie A. Kolodziejski, Dr. Gale S. Petrich, Principal Research Scientist

Graduate Students
Reginald E. Bryant, Alex J. Grine, Sheila Nabanja, Orit Shamir, Ta-Ming Shih, Ryan D. Williams

Technical and Support Staff
Tiffany Kuhn

Introduction

The emphasis of our research program is the design, epitaxial growth, device fabrication and characterization of a number of photonic and opto-electronic structures and devices. The epitaxial growth of the heterostructures is performed in a Veeco GEN 200 solid source, dual-reactor molecular beam epitaxy (MBE) system. The Veeco MBE system is capable of the epitaxial growth of dilute nitrides and antimony-based films in addition to arsenide- and phosphide-based films. The system platens hold multiple 2”, 3" or 4" wafers, or a single 6" or 8" wafer. The system incorporates a low wobble manipulator that will enable in-situ feedback control of the epitaxial processes using optical sensors such as band edge absorption spectroscopy and spectroscopic ellipsometry.

In the following sections, the status of the various research projects will be discussed. Projects include the development and simulation of rudimentary optical logic gates, the development of optical modulators for operation at 800nm, the development of saturable Bragg reflectors for short pulse lasers, the development of Si-based two-dimensional photonic crystal super-collimators, the development of an electrically-activated nanocavity photonic crystal laser and the development of high index contrast optical switches. These projects are collaborative efforts of multiple professors at MIT and members of the MIT Lincoln Laboratory technical staff in order to successfully design, simulate, fabricate and characterize the aforementioned optical devices.

1. Photonic Integrated Circuits for Ultrafast Optical Logic

Sponsors
Defense Advanced Research Projects Agency: Contract Number: W911NF-06-1-0060

Project Staff
Ryan D. Williams, Dr. Gale S. Petrich, Professor Rajeev Ram, Professor Erich P. Ippen, Professor Leslie A. Kolodziejski, and Dr. Scott Hamilton

The aim of this project is to model and to produce a modular monolithically-integrated all-optical unit cell capable of performing a complete set of Boolean operations at speeds of 100s of gigabits per second. Optical logic operations, wavelength conversion, and other advanced optical switching schemes can be implemented using the design. The basic structure consists of a balanced Mach-Zehnder interferometer (Figure 1) with an InGaAsP-based semiconductor optical amplifier in each arm. By investigating the device design and fabrication tolerances using the beam propagation method and finite-difference time-domain techniques, the critical device dimensions were modeled prior to fabrication.

Fabrication processes have been developed to create the all-optical logic unit cell. The waveguide design calls for the vertical integration of passive waveguides and active amplifiers. Using an adiabatic taper coupler (Figure 2), the optical mode is transferred between the lower passive waveguide and the upper active waveguide of the twin-waveguide structure. To minimize the amount of InGaAsP material being etched, the waveguides are placed in the center of a trench as seen in the figures. Complete optical logic structures have been fabricated as shown in Figure 3. In addition to the optical logic unit cell, isolated components have been fabricated and are being tested to confirm the device design and the computer simulation results.

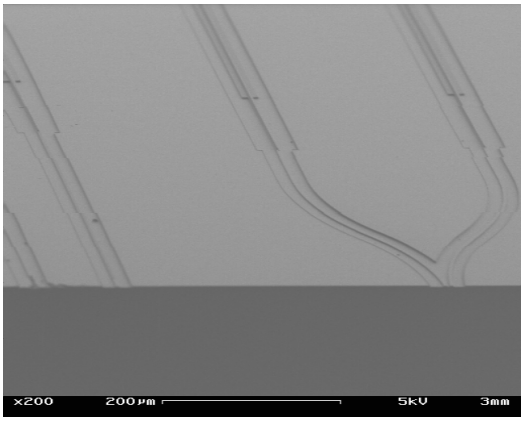

Figure 1. A scanning electron micrograph of the beginning region of the Mach-Zehnder interferometer (MZI) that is the basis for the optical logic unit cell. By controlling the balance of the semiconductor optical amplifiers in each arm of the MZI, basic Boolean functionality can be achieved.

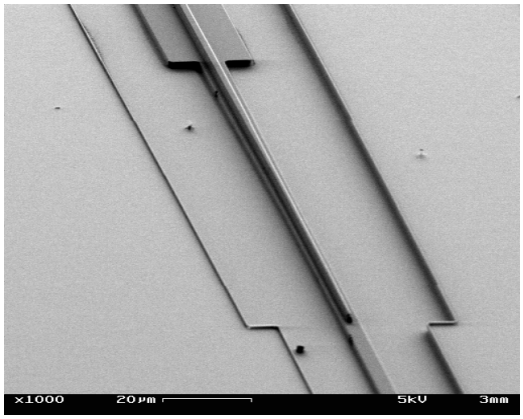

Figure 2. A scanning electron micrograph showing the active waveguide taper that is used to transfer the optical mode between the lower passive waveguide (lower right) and the upper active waveguide (upper left).

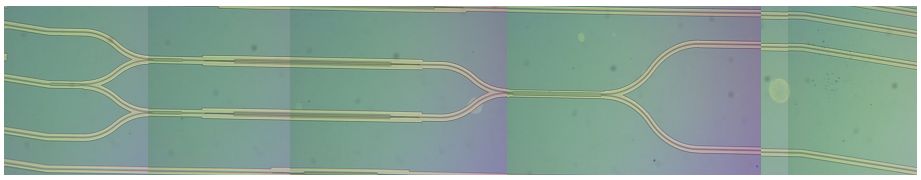

Figure 3. The optical logic unit cell is capable of Boolean operations and wavelength conversions forming the basis for more advanced optical logic and switching schemes. Total device length is approximately 5 mm.

2. Ultra Broad Band Modulator Arrays

Sponsors
Defense Advanced Research Projects Agency: Contract Number: W911NF-06-1-0060

Project Staff
Orit Shamir, Dr. Gale S. Petrich, Professor Franz X. Kaertner, Professor Erich P. Ippen and Professor Leslie A. Kolodziejski

Creating an arbitrary optical waveform at wavelengths that are centered at 800nm requires an ultra broad band modulator array. Since these modulators are required to operate around 800nm, the material choices are limited to relatively high Al content AlGaAs and to $In_{0.5}(Ga_xAl_{1-x})_{0.5}P$ layers lattice-matched to GaAs. In addition, since GaAs absorbs light with a wavelength less than 870nm, the lower cladding layer of the modulator must be relatively thick to isolate the modulator from the GaAs substrate. To create the largest mode possible and to minimize the coupling loss, the index contrast between the waveguiding layers and the cladding layers should be minimized. Hence, a dilute waveguide structure in which thin layers of high index material are embedded in a low index material is employed. The resulting layered structure has an effective index slightly higher than the low index material and is determined by the layer thicknesses as well as the refractive index of the two materials that comprise the dilute waveguide. However, if the dilute waveguide is not completely etched, due to the low index contrast of the dilute waveguides, the bending radius is quite large, on the order of a millimeter.

The first modulator that is being fabricated is an arsenide-based structure that is designed to be single mode with a 2 micron wide ridge waveguide. Using OptiBPM, the fundamental mode for the arsenide-based modulator is roughly 2 μm x 1μm (WxH). The structure, grown by molecular beam epitaxy, is an $Al_{0.8}Ga_{0.2}As$-based structure in which the dilute waveguide consisted of alternating layers of $Al_{0.8}Ga_{0.2}As$ and InGaP. The structure is challenging in terms of the epitaxial growth; although the use of $Al_{0.8}Ga_{0.2}As$ for the cladding layer minimized the lattice-mismatch problem, achieving high quality, high Al content AlGaAs cladding layers is difficult due to the low Al adatom mobility on the surface during growth. To minimize free carrier loss, P-I-N structures are employed in which the concentration of the Si and Be dopants were graded from the contact layers to the dilute waveguide region. Photoluminescence (PL) measurements from the arsenide-based structure show a weak PL peak at ~650nm from the InGaP layers in the dilute waveguide. The $Al_{0.8}Ga_{0.2}As$ layers have an indirect band gap and hence do not exhibit photoluminescence. Due to the high etch selectivity between the arsenide and phosphide layers, the uppermost high index layer of the dilute waveguide also acts as an etch stop.

In addition to this original structure, a second MOS-type structure has also been grown which differs from the previous design by the addition of two AlAs layers that can be subsequently oxidized into Al_xO_y, enabling a strongly confined optical mode in the middle of the structure. In addition, the added Al_xO_y layers will allow the device to be capable of withstanding higher operating voltages without concern of breakdown or carrier loss. Furthermore, the device can be unipolar. The structure also contains an InAlP etch stop to facilitate fabrication.

A mask set suitable for both structures has been designed and fabricated. The mask set contains Mach Zehnder interferometer modulators of various lengths with multimode interference couplers or Y-splitters as seen in Figures 1 and 2, respectively. The Mach Zehnder interferometer modulators as well as conventional modulators are oriented both parallel and perpendicular to the major flat of the 2” GaAs(100) wafers. The mask set also contains a variety of passive components such as Y-splitters, multimode interference couplers as well as straight and curved waveguides. The mask set for the reverse-biased P-I-N diode modulators that were described previously can also be used for the MOS-type modulators. The only difference in the fabrication process is the addition of the AlAs oxidation step that is inserted after the reactive ion etching step that is used to define the waveguides.

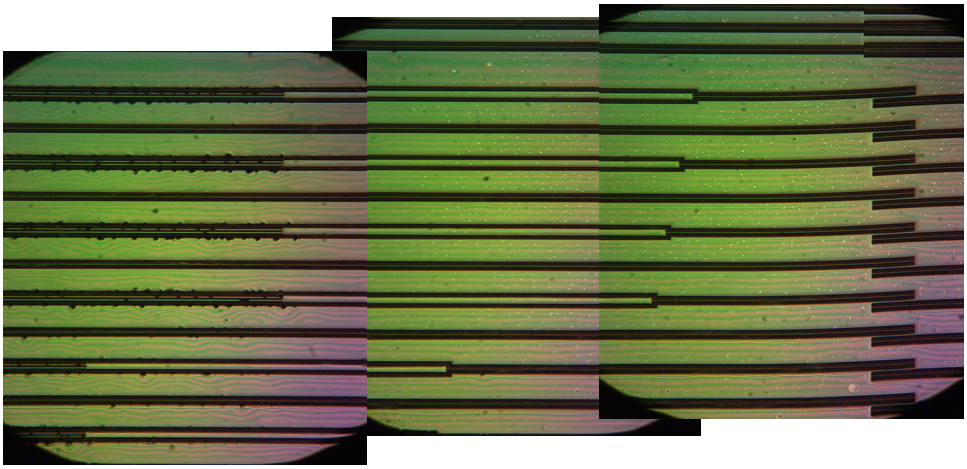

Figure 1. Micrograph images of multi-mode interferometers fabricated in the arsenide-based structures.

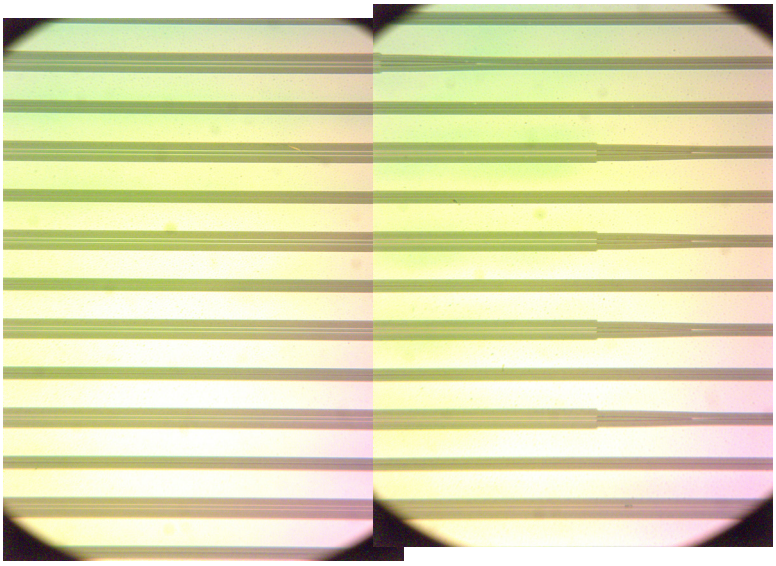

Figure 2. Composite micrograph image of InGaP/AlGaAs Y-splitters

3. Saturable Bragg Reflectors for Modelocking Ultrafast Lasers

Sponsor
National Science Foundation, Award Number ECS-0322740
Office of Naval Research, Contract Number N00014-02-1-0717
Q-PEAK PO51843
Defense Advanced Research Projects Agency: Contract Number 4R0011-05-C-0155

Project Staff:
Dr. Gale S. Petrich, Professor Franz X. Kaertner, Professor Erich P. Ippen and Professor Leslie A. Kolodziejski

A variety of saturable Bragg reflectors (SBRs) were grown, by molecular beam epitaxy (MBE), for use in an Er-Yb laser. For each SBR, the final structure was achieved using two separate MBE growth steps. The base mirror substrate (used for each of the SBRs) was grown on multiple 2 inch GaAs wafers simultaneously; the base mirror substrate is comprised of 20 ¾ pairs of $Al_{0.95}Ga_{0.05}As$ and GaAs with the uppermost surface being a λ/8n-thick (n is the refractive index) layer of GaAs. On top of the base mirror substrate and in separate growths for each SBR, four additional mirror pairs of $Al_{0.95}Ga_{0.05}As$ and GaAs starting with a λ/8n-thick GaAs layer were deposited along with a particular λ/2n-thick saturable absorber section. The saturable absorber sections contain either one or two InGaAs quantum well(s); the InGaAs quantum wells are clad with either GaAs or InP. The various SBRs are shown schematically in Figure 1. The use of two λ/8n-thick GaAs layers allows the resulting re-growth interface to reside in the middle of a GaAs layer. The benefit of such a GaAs-GaAs re-growth scheme is two-fold: (i) if the base mirror substrate growth is terminated on an $Al_{0.95}Ga_{0.05}As$ surface, the removal of the native $Al_{0.95}Ga_{0.05}As$ oxide in the re-growth step is extremely difficult and would lead to a overlayer with poorer microstructural quality; and (ii) if the base mirror substrate growth is terminated on a λ/4n-thick GaAs layer, in the re-growth step the resulting heteroepitaxial GaAs-$Al_{0.95}Ga_{0.05}As$ interface may exhibit a higher degree of surface roughness (certainly greater surface roughness than the first GaAs-$Al_{0.95}Ga_{0.05}As$ interface obtained when using the GaAs-GaAs re-growth scheme). The resulting increased surface roughness of such an SBR is expected to increase the non-saturable loss.

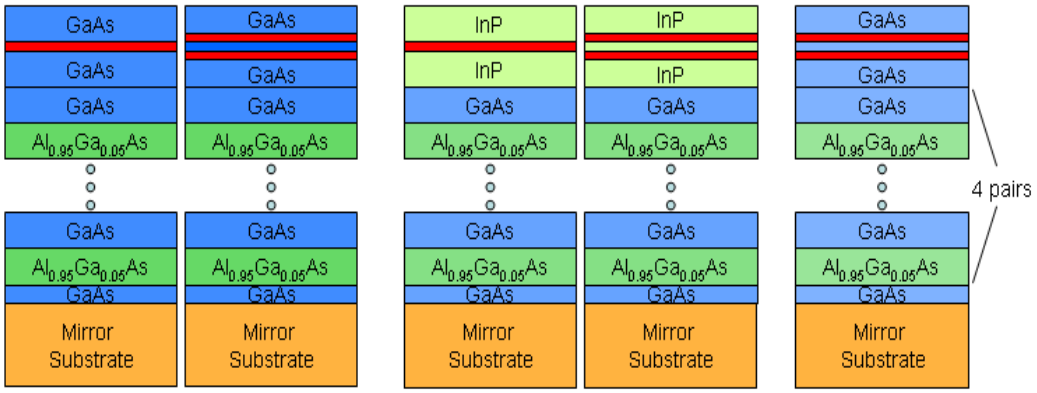

Figure 1. Schematic diagrams of the various saturable Bragg reflectors that were grown on a base mirror substrate. The red layer represents the InGaAs quantum well.

The reflectivity characteristics of the different saturable Bragg reflectors were assessed. Figure 2 shows the measured reflectivity spectra of four different SBRs having one or two quantum wells and clad by either GaAs [Fig. 2(a)] or InP [Fig. 2(b)] layers. As expected, as the number of InGaAs quantum wells increased from one to two, the overall reflectivity decreased due to the absorption of light within the additional InGaAs quantum well. In addition, the effect of

having mirror layers with smaller layer thickness than designed during the re-growth of the GaAs-based absorbers and the upper-most mirror layers is apparent on the short wavelength side of the reflectivity spectra as shown in Fig. 2(a).

Although the SBRs were designed to mode-lock the laser, only one of the SBRs actually mode-locked the laser. The two SBRs with InP cladding layers and the SBR with a single quantum well with GaAs cladding layers exhibited both Q-switching as well as mode-locking. The two SBRs with two InGaAs quantum wells with GaAs cladding layers should yeild similar results, however, only one of the samples successfully mode-locked the laser. Further optical measurements of the SBRs are underway.

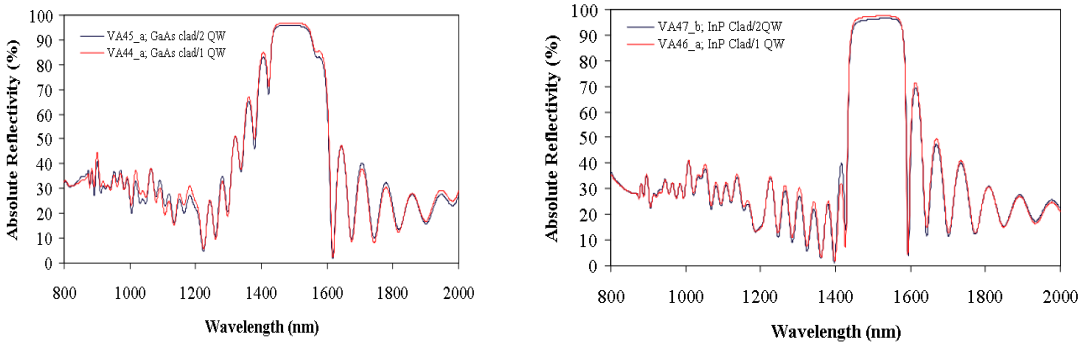

Figure 2a) The reflectivity spectra of the SBRs with one and two InGaAs quantum wells clad with GaAs. b) The reflectivity spectra of the SBRs with one and two InGaAs quantum wells clad with InP. All four SBR structures were grown on the base mirror substrate.

4. Super-collimation of Light within Photonic Crystal Slabs

Sponsor
National Science Foundation Award Number DMR-02-13282
MARCO Interconnect Focus Center, Subcontract from Georgia Institute of Technology
Contract Number B-12-M06-52
STTR Contract Number

Project Staff
Andre Kurs, Ta-Ming Shih, Marcus Dahlem, Dr. Gale S. Petrich, Professor Marin Soljacic, Professor Erich P. Ippen, Professor Leslie A. Kolodziejski, Dr. Katherine Hall and Dr. Morris Kessler

Super-collimation is the divergentless propagation of a light beam that occurs when the light beam is guided by the dispersion properties of a photonic crystal (PhC) rather than by defects or traditional waveguiding structures. Photonic crystals are dielectric structures that exhibit periodicity of their dielectric constant in one, two, or three dimensions. Successful fabrication and measurement of super-collimation has been performed previously for a two-dimensional PhC composed of a square lattice of cylindrical holes etched into silicon. Super-collimation for more than 600 isotropic diffraction lengths has been observed for this device.

The current goal of the research is to demonstrate super-collimation with a two-dimensional PhC that is composed of a square lattice of cylindrical silicon posts, rather than holes. The initial design has focused on realizing super-collimation at a wavelength of 1530 nm corresponding to a lattice constant, post radius, and Si thickness of 437.5 nm, 250 nm and 700 nm, respectively. Two fabrication processes have been developed and tested. The device has been fabricated using a silicon-on-insulator wafer in which the low-index silicon dioxide layer (3 μm thick) is used to minimize radiation loss into the high-index silicon substrate. The Si posts are patterned with interference lithography using a HeCd ultraviolet (325nm) laser. The pattern is transferred via reactive ion etching (RIE). The RIE chemistries and other parameters are optimized to increase uniformity and to decrease sidewall roughness. The two fabrication methods are mainly distinguished by the RIE chemistry with which Si posts are etched: Cl_2 versus CF_4. Figure 1 is a scanning electron microscope image of a finished device fabricated with the Cl_2 Si-etch method. The Si posts exhibits a slightly tapered geometry and when the taper was incorporated into the simulation, the simulation suggests that super-collimation still occurs. Optical testing of the finished devices is underway.

Perturbation theory calculations show that a super-collimator based on the rod design is more sensitive than a super-collimator based on the hole design to changes in the index of refraction of the medium in the holes or between the rods. This improved sensitivity suggests that the rod-based super-collimator design is an excellent candidate for chemical sensing applications.

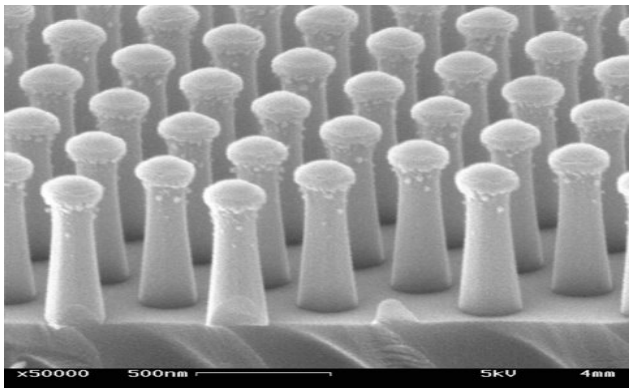

Figure 1. SEM image of the super-collimator fabricated with the Cl_2-based reactive ion etching. The silicon posts are 700 nm tall and reside on a 3 μm thick layer of silicon dioxide on a silicon wafer. The SiO_2 etch mask is on top of the Si posts.

5. Electrically-Activated Nanocavity Laser using One-Dimensional Photonic Crystals

Sponsors
National Science Foundation: Award Number DMR-02-13282

Project Staff
Alex J. Grine, Sheila Nabanja, Dr. Gale S. Petrich, and Professor Leslie A. Kolodziejski

An electrically-activated nanocavity laser, that is capable of being integrated within photonic integrated circuits, is being developed. The laser employs two crossed members with embedded one-dimensional photonic crystals in order to create an optical cavity at the intersection. To achieve electrical activation, one of the cross members is doped p-type and the other doped n-type. Hence, a PN-junction is formed at the intersection of the two cross members. Furthermore, by adjusting the thickness of the individual cross members, one of the cross members is designed to act as a single mode waveguide. By adjusting the reflectivities of the photonic crystals, the light that is generated within the nanocavity, will be directed towards the desired output waveguide. The electrically-activated nanocavity laser is shown schematically in Figure 1.

The fabrication of the electrically-activated photonic crystal laser is underway. Two lithography techniques are being employed; conventional contact lithography is used for the features with dimensions greater than 1 micron, while electron beam lithography is used to define the submicron-sized features. Figure 2 shows a micrograph of the contact pads and wires for 12 lasers on the wafer that is currently being processed. The actual nanocavity portion of the lasers has not been defined yet.

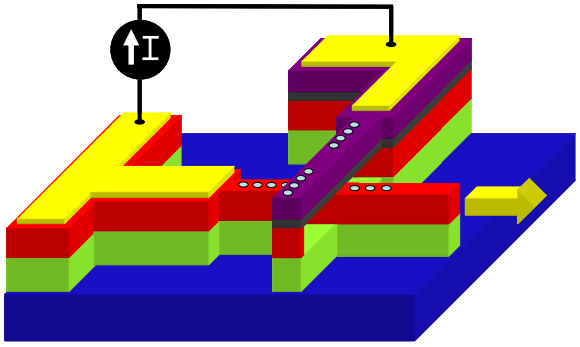

Figure 1. Schematic of the electrically-activated, photonic crystal nanocavity laser. The yellow arrow represents the direction and location of the emitted light.

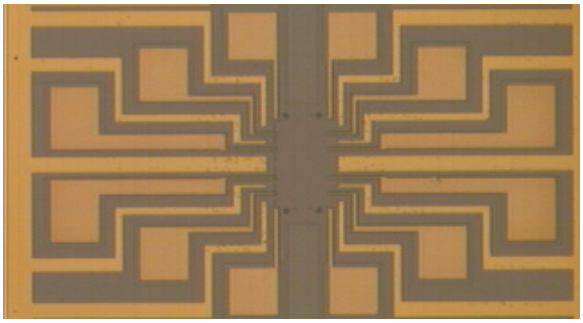

Figure 2. A micrograph of the contact pads and wiring for 12 lasers on a wafer that is currently being processed.

6. A Nanoelectromechanically Tunable High-Index-Contrast Interference Directional Coupler

Sponsors:
National Science Foundation Award Number DMR-02-13282

Project Staff
Reginald E. Bryant, Dr. Gale S. Petrich, and Professor Leslie A. Kolodziejski

Designs that utilize nanoprecision electrostatic mechanical actuation are likely to improve fabrication tolerances for evanescently-coupled, channel waveguide devices. Evanescent couplers, or directional couplers (DC), are notorious for their sensitivity to fabrication irregularities due mainly to the exponential dependence of the evanescent coupling on the waveguide-to-waveguide separations. A design that incorporates growth and fabrication precision as well as electromechanical nanodisplacements can significantly increase fabrication tolerances.

Molecular beam epitaxial (MBE) growth precisely defines channel waveguide heights. MBE growth is capable of depositing homogeneous layers of material with minimal interdiffusion. Precise channel waveguide separations are achieved by a combination of atomic layer deposition (ALD) of low-index-contrast (LIC) material and nanoelectromechanical (NEM) actuation. ALD LIC films can uniformly coat features one monolayer at a time, thus precisely defining a waveguide-to-waveguide separation with the coating thicknesses. NEM actuation establishes intimate contact between the two ALD LIC-coated high-index-contrast channel waveguides. NEM directional coupler waveguides are only sensitive to fabrication width variations. Optimized DC design can reduce the effect these variations have on the NEM DC.

The NEM-DC waveguides are initially set in an off-resonance state (Figure 1), and are then deflected into an on-resonance state via the application of V_0 volts (Figure 2). The initial off-resonance NEM-DC design scheme allows the waveguides to be lithographically-defined as isolated features. All features can also be arranged with separations similar to the waveguide-to-waveguide off-resonance separations without having an optical loss penalty. This arrangement reduces lithographic proximity effects and loading effects associated with species-diffusion based fabrication processes (Reactive Ion Etching, and Oxidation).

Upon being deflected into an on-resonance state (V_0 volts), the two waveguides are brought into mechanically strained intimate contact. Should there be any deviations in width; the separation is preserved by the thickness of the LIC ALD coating. Depending on the application, the static power needed to preserve the strained intimate contact can be removed with the use of mechanical latches.

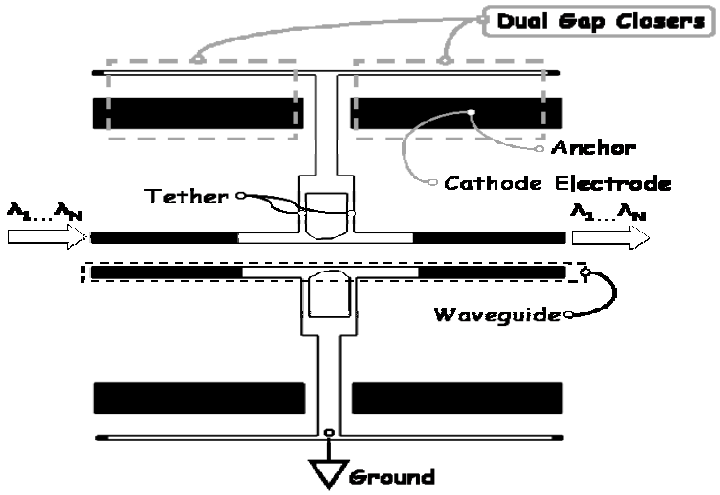

Figure 1. Top-view schematic of the directional coupler in the unpowered state. The optical signal remains in the upper waveguide.

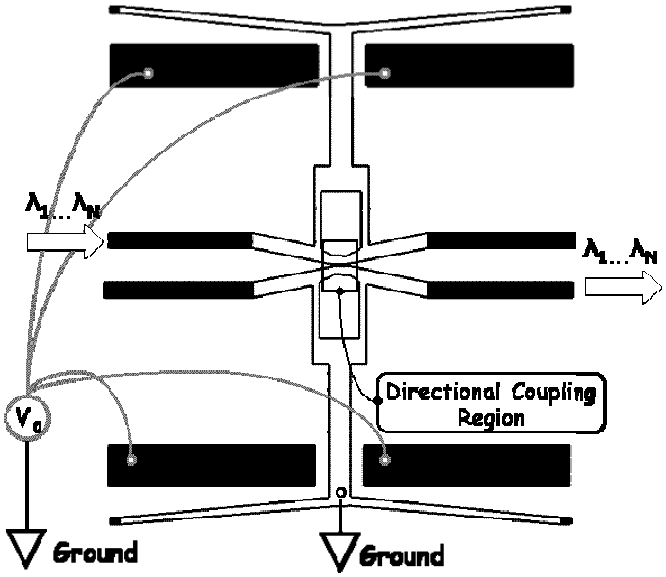

Figure 2. Top-view schematic of the directional coupler in the powered state. The optical signal is coupled into the lower waveguide as the two waveguides are brought into close proximity to allow for optical coupling.

Publications

Journal Articles, Published

P.T. Rakich, M.S. Dahlem, S. Tandon, M. Ibanescu, M. Soljacic, G.S. Petrich, J.D. Joannopoulos, L.A. Kolodziejski, E.P. Ippen, ”Achieving centimetre-scale supercollimation in a large-area two-dimensional photonic crystal” *Nature Materials*, 5(2): 93-6 (2006).

Theses

A. Grine, *The Design and Fabrication of an Electrically-Activated Photonic Crystal Microcavity Laser*, M. S. Thesis, Department of Electrical Engineering and Computer Science, MIT, 2007.